Articles

Crystal Structure of Neurotrophin-3 Homodimer Shows Distinct Regions Are Used To Bind Its Receptors[†,‡]

Manish J. Butte,[§] Peter K. Hwang,[||] William C. Mobley,[⊥] and Robert J. Fletterick*[,||]

Graduate Group in Biophysics and Department of Biochemistry and Biophysics, University of California, San Francisco, Box 0448, San Francisco, California 94143, and Department of Neurology, Stanford University, Palo Alto, California 94304

Received May 26, 1998

ABSTRACT: Neurotrophin-3 (NT-3) is a cystine knot growth factor that promotes the survival, proliferation, and differentiation of developing neurons and is a potential therapeutic for neurodegenerative diseases. To clarify the structural basis of receptor specificity and the role of neurotrophin dimerization in receptor activation, the structure of the NT-3 homodimer was determined using X-ray crystallography. The orthorhombic crystals diffract to 2.4 Å, with dimer symmetry occurring about a crystallographic 2-fold axis. The overall structure of NT-3 resembles that of the other neurotrophins, NGF and BDNF; each protomer forms a twisted four-stranded β sheet, with three intertwined disulfide bonds. There are notable differences, however, between NT-3 and NGF in the surface loops and in three functionally important regions, shown in previous mutagenesis studies to be critical for binding. One such difference implies that NT-3's binding affinity and specificity depend on a novel hydrogen bond between Gln 83, a residue important for binding specificity with TrkC, and Arg 103, a residue crucial for binding affinity with TrkC. NT-3's extensive dimer interface buries much of the otherwise solvent-accessible hydrophobic surface area and suggests that the dimeric state is stabilized through the formation of this hydrophobic core. A comparison of the dimer interface between the NT-3 homodimer and the BDNF/NT-3 heterodimer reveals similar patterns of hydrogen bonds and nonpolar contacts, which reinforces the notion that the evolutionarily conserved neurotrophin interface resulted from the need for receptor dimerization in signal initiation.

Neurotrophin-3 (NT-3)[1] is a protein growth factor that belongs to the neurotrophin family, which includes nerve growth factor (NGF), brain-derived neurotrophic factor (BDNF), neurotrophin-4 (also called neurotrophin-4/5), and neurotrophin-6. Neurotrophins act on specific developing neuronal populations to prevent or direct programmed cell death, promote differentiation, and regulate proliferation (*1*). In addition, neurotrophins act in the mature nervous system to maintain neuronal function (*2*), enhance neuronal function in animal models of neurological diseases (*3*), and may play a role in neural tumor progression (*4*). The neurotrophins belong to the cystine knot superfamily, a large group that shares a conserved core of three intertwined disulfide bonds. Other members of this family include platelet-derived growth factor (PDGF), transforming growth factor β (TGF-β), and human choriogonadotropin (hCG). All cystine knot growth factors are nonglobular β-sheets, lacking a well-defined hydrophobic core. In addition, they all exist exclusively as dimers, the interface of which is notable for its extensive buried hydrophobic surface. One hypothesis suggests that dimerization is required because the protomers alone are not structurally stable. Only upon dimerization is there a sufficient hydrophobic core to stabilize the structure (*5*). The NGF crystal structure supports this notion, but whether it applies to NT-3 or the other neurotrophins was uncertain.

At least two NT-3 cell surface receptors have been identified. TrkC, a receptor tyrosine kinase that shows selectivity and nanomolar affinity for NT-3, must be activated for the normal survival of certain peripheral nervous system and sensory neurons (*6*). $p75^{NTR}$, a member of the tumor necrosis factor receptor (TNFR) superfamily, binds all the neurotrophins with nanomolar affinity and plays a role in neuronal apoptosis (*1*). Extensive mutagenesis has defined the sequences in NGF (*7*−*10*) and NT-3 (*11*) that mediate

[†] This work is supported by the Office of Naval Research predoctoral fellowship (to M.J.B.), the McGowan Charitable Fund (to W.C.M.), and NIH Grant DK32822 (to P.K.H. and R.J.F.).

[‡] Atomic coordinates have been deposited with the Brookhaven Protein Data Bank as 1nt3.

* Corresponding author. Phone: 415-476-5080. Fax: 415-476-1902. E-mail: flett@msg.ucsf.edu.

[§] Graduate Group in Biophysics, UCSF.

[||] Department of Biochemistry and Biophysics, UCSF.

[⊥] Department of Neurology, Stanford University.

[1] Abbreviations: NT-3, neurotrophin-3; BDNF, brain-derived neurotrophic factor; NGF, nerve growth factor; PDGF, platelet-derived growth factor; TGF-β, transforming growth factor β; hCG, human choriogonadotropin; TNFR, tumor necrosis factor receptor.

10.1021/bi981254o CCC: $15.00
Published on Web 11/12/1998

binding affinity and specificity for their receptors. One puzzling conclusion is that each neurotrophin uses wholly different sequences to bind its receptors. Whether common themes may be apparent in the spatial arrangement of these residues is not yet known. Even more oddly, NT-3 is the only neurotrophin that can bind, albeit weakly, to the other Trk receptors, TrkA and TrkB (the cognate receptors for NGF and BDNF, respectively); the biological significance of this has not been established. In contrast to the promiscuity of its cognate ligand, TrkC is very stringent: it binds only NT-3. Are there structural clues to NT-3's binding specificity?

To explore NT-3's structural relationship with the other neurotrophins and cystine knot growth factors and to investigate the structural basis for receptor specificity, we determined the structure of the NT-3 homodimer using X-ray crystallography. The NT-3 protomer from the structure of a BDNF/NT-3 heterodimer (*12*) was used as a search model for molecular replacement phasing. The structure of the recombinant human NT-3 homodimer was compared to the NGF homodimer and the BDNF/NT-3 heterodimer. We propose a structural model for how NT-3 binds to TrkC and $p75^{NTR}$. Our results also support a simple structural explanation for obligate dimerization of the neurotrophins.

EXPERIMENTAL PROCEDURES

Protein Purification and Crystal Growth. Recombinant human NT-3 was expressed in *Escherichia coli* and purified to greater than 95% purity by Amgen, Inc., and donated to us by Regeneron Pharmaceuticals. NT-3 was buffered in Tris-HCl, pH 8.0, and concentrated to 15 mg/mL. Edman sequencing from the N-terminus to Val 13 and silver-stained SDS−PAGE were performed to ensure the protein's identity. Crystals were grown by vapor diffusion from a reservoir solution of 200 mM ammonium sulfate, 32% PEG 400, and 100 mM MES [2-(*N*-morpholino)ethanesulfonic acid] at pH 5.6, which was optimized from starting conditions appearing in refs *13* and *14*. The crystals appeared as thin plates and grew to their full size (approximately 0.1 mm in the largest dimension) in about 1 week at 18 °C.

Data Collection and Processing. A crystal was captured in a nylon loop and transferred to a 15% glycerol/85% reservoir cryoprotectant solution briefly and then rapidly frozen in a liquid nitrogen bath. A 2.4 Å data set (half the reflections have an I/σ of 3.0 at 2.4 Å resolution) was measured from a single crystal at Stanford Synchrotron Radiation Laboratory (SSRL) beamline 7-1, with an average coverage of 85.3% to 2.4 Å (89.6% for the 2.5−2.4 Å shell). The space group is $P2_12_12$, and the unit cell has parameters $a = 37.4$ Å, $b = 52.1$ Å, and $c = 64.8$ Å. The intensity data were processed and integrated with DENZO and Scalepack (*15*). Statistical analysis of the intensities with a Wilson plot [CCP4 program Wilson (*16*)] revealed a mean isotropic temperature factor of 33 $Å^2$.

Molecular Replacement. The structure was solved by molecular replacement, using the NT-3 protomer from the BDNF/NT-3 heterodimer structure (PDB 1bnd) (*12*) as the search model. This search model was chosen because it should have 100% identity to our NT-3, except for two inconsistencies in the PDB entry: Val 11 should be a Tyr and Gln 44 should be a Gly according to the Swiss-Prot entry for human NT-3 (accession P20783) and according to the results of our N-terminal sequencing experiment. All 108 residues from the NT-3 protomer of the heterodimer structure were used, including all side chains. A number of candidate solutions were found with the CCP4 program AMoRe (*17*). The top solutions were visualized in a unit cell using INSIGHT II (version 95.0, Biosym Technologies, San Diego, CA), and the second solution was found to have the best appearance, in terms of both packing with its symmetry mate and global similarity to the search model. The dimer mate falls across a crystallographic 2-fold symmetry axis. For this solution, the R_{cryst} was 41.6% and the correlation coefficient was 59.7.

Refinement. The molecular replacement solution model underwent a rigid-body minimization and a Cartesian simulated annealing during which a bulk solvent correction was applied. Repeated cycles of refinement using X-PLOR (*18*) and the developmental CNS (Crystallography and NMR System) program (A. T. Brunger, personal communication) and manual rebuilding using MOLOC (*19*) followed to ensure that the free *R*-factor decreased steadily. Refinement included positional refinement, Cartesian and torsional simulated annealing, and *B*-factor refinement with the maximum likelihood target (*20*). The model was refined against 90% of the measured data between 30.0 and 2.4 Å using the Engh and Huber stereochemical dictionary. The remaining 10% of the data were excluded from all refinement calculations to cross-validate the progress of refinement (the free *R* set).

After 20 cycles of refinement and manual rebuilding, water molecules were added to the structure provided that (1) density appeared $>2.0\ \sigma$ on the $2F_o - F_c$ map, (2) they formed hydrogen bonds of reasonable geometry, and (3) their inclusion reduced the free *R*-factor. The refinement continued with 2.0 σ or better structure factors in the 8.0−2.4 Å resolution range to reduce the effects of poorly measured low-resolution data. In later stages, solvent-flipped electron density maps were calculated using the CCP4 program SOLOMON (*21*). Phase probabilities from SOLOMON were also used as constraints in the MLHL target function (N. S. Pannu et al., *Acta Crystallogr., Sect. D*, in press) implemented in CNS; this reduced the free *R*-factor further.

Many loop regions of the protomer had only sparsely visualizable density in a simulated annealing omit map, notably at the residues between 42 and 47, between 61 and 66, between 68 and 71, and between 93 and 95. A few residues at the N- and C-termini (8−10 and 115) also show poor electron density because they are inadequately constrained. To improve the electron density maps of these loops, we attempted multicrystal averaging with a lower resolution data set (good to 3.2 Å) collected from a similar crystal, using the program MAVE (*22*). This did not significantly improve the density in the loops and in fact suggested that the above loops may assume variable conformations. Many of the above loop regions were also noted to be disordered or variable in conformation in the two different NGF structures (*23*, *24*) and in the BDNF/NT-3 heterodimer. Unfortunately, these disordered loop regions make up around 20% of the atoms of the protomer, so the *R*-factor and free *R*-factor are somewhat higher than might be expected for a similarly sized, globular protein. Fortunately, all the residues that appear to play a biological role

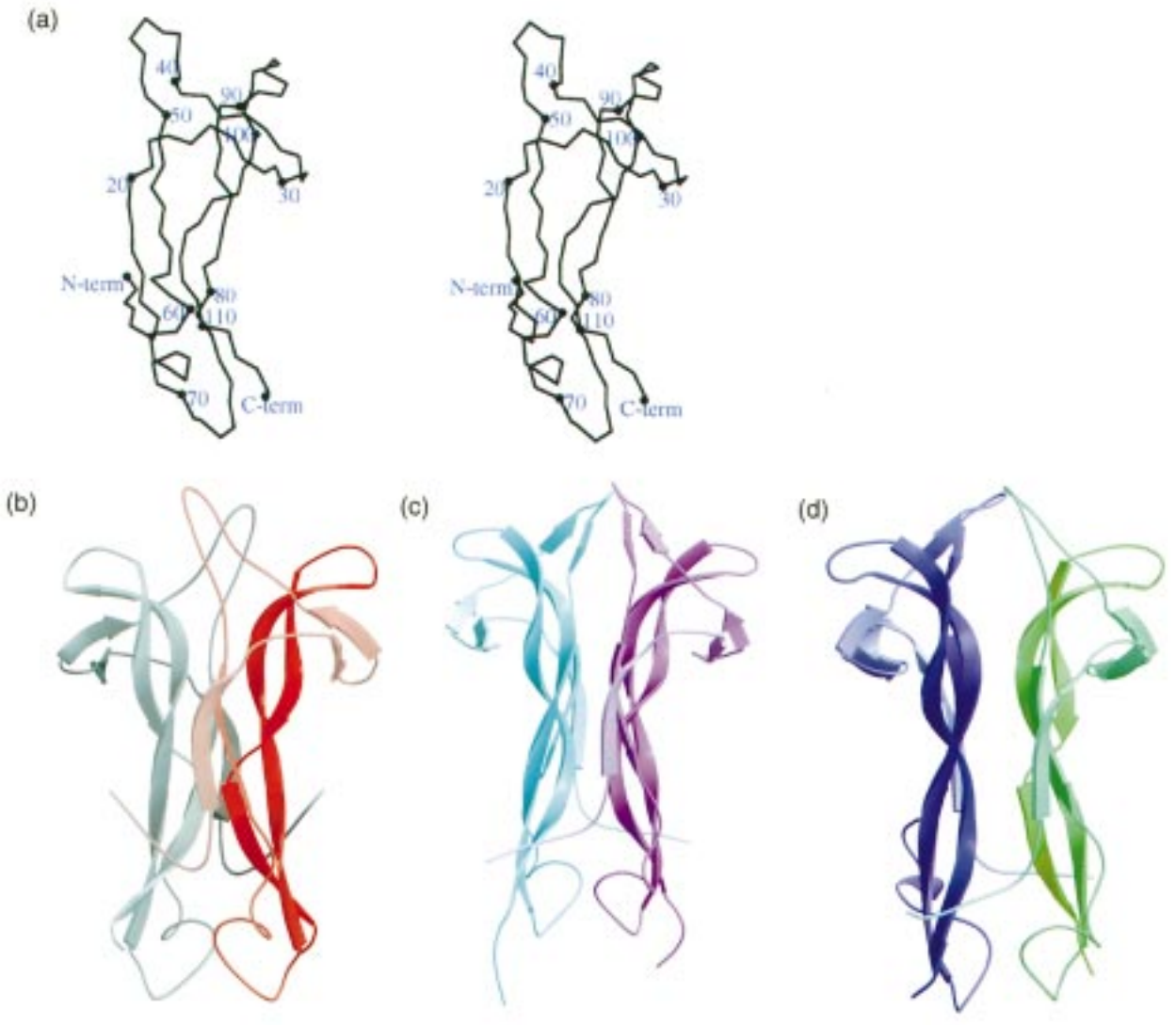

FIGURE 1: NT-3 shares a similar fold with NGF and the BDNF/NT-3 heterodimer. (a) Stereo diagram of the α-carbon trace of the protomer. The three known neurotrophin structures, (b) NT-3 homodimer, (c) NGF dimer, and (d) BDNF/NT-3 heterodimer, with BDNF in purple and NT-3 in green.

in mediating receptor binding were well ordered, as will be discussed below. The final *R*-factor was 23.3 and the free *R*-factor was 26.7, with excellent geometry (for all data, the *R*-factors were less than 1% higher). A Ramachandran plot reveals 97% of the residues fall into allowed regions, with the only exceptions being residues in the aforementioned loops. The overall statistics for data collection and refinement are summarized in Table 3. To check for search model bias, a high-temperature electron density omit map was calculated, a representative portion of which is shown in Figure 5. It revealed that the main chain positions were similar between our structure and the search model and that the side chain conformations clearly support our structure versus that of the search model.

Analysis. The dimer interface statistics in Table 2 and the accessible surface area calculations were computed using the ASC program (*25*), using a 1.4 Å probe. Molscript (*26*), Raster3D (*27*), and GRASP (*28*) were used to view the final structure and produce the figures. The program ALSCRIPT (*29*) was used for display of the sequence alignment. Superimposed neurotrophin structures were compared using the LSQMAN program (*30*).

Table 1: Root Mean Square Differences (Å) in Cα Superpositions[a]

	target for superposition		
reference	NT-3	NT-3/BDNF	NGF
NT-3		1.02 (198)	1.20 (200)
NT-3/BDNF	0.30		0.95 (202)
NGF	0.31	0.20	

[a] Values above the diagonal are root mean square differences comparing the superpositions of α-carbons (number of carbons used in the alignment is in parentheses) of the various neurotrophin dimers. Values below the diagonal represent the same for the six cysteine residues in each of those structures.

RESULTS AND DISCUSSION

Overall Structure. The NT-3 dimer shares a similar fold with NGF and the BDNF/NT-3 heterodimer (Figure 1). The protomer tertiary structure consists of four antiparallel β strands, with the fourth β strand twisted around the third, a feature conserved across all the cystine knot growth factors (*5*). The three disulfides that make up the cystine knot are virtually superimposable on those of NGF with a rms deviation of less than 0.3 Å (Table 1). They follow the pattern established in all cystine knot growth factors:

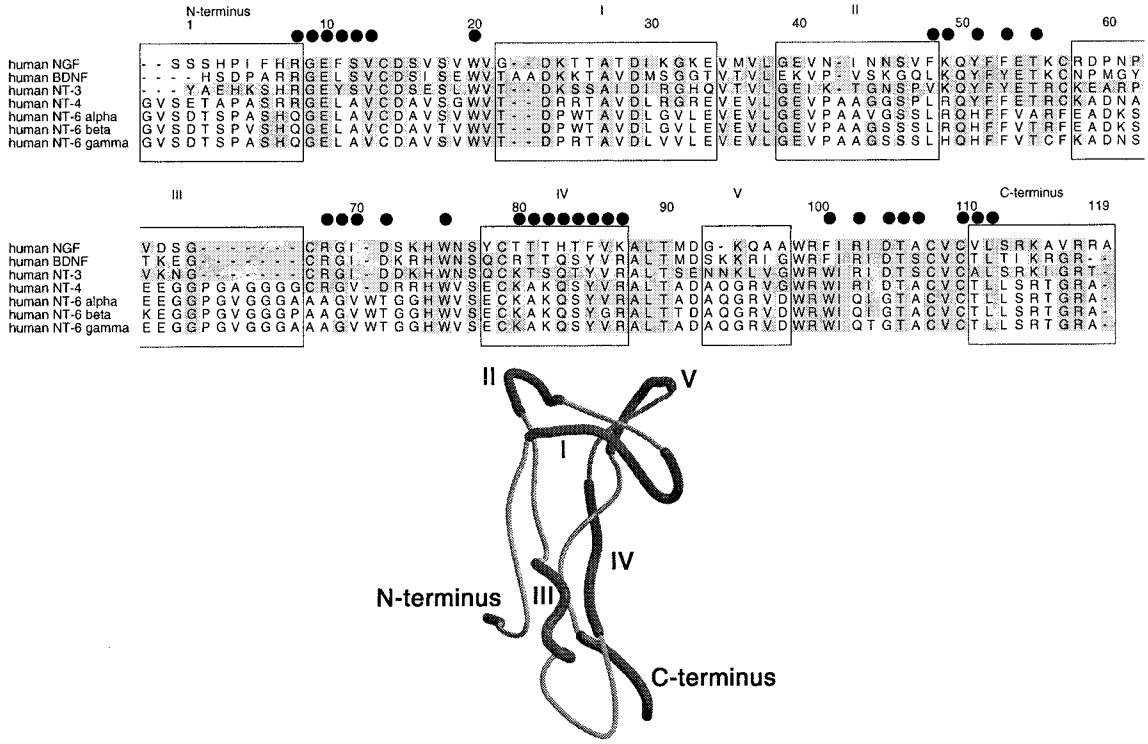

FIGURE 2: Sequence alignment of NT-3 with other known human neurotrophins: NGF, BDNF, NT-4, and three NT-6 sequences (GenBank accession numbers M37763, M21062, M37762, M86528, S41522, S41540, and S41541, respectively). The residue numbering is based on NT-3. The black circles represent residues in NT-3 that are in the dimer interface. The roman numerals identify the variable regions of the sequence alignment with the structure.

Cys(III−VI) penetrates the ring formed by Cys(I−IV) and Cys(II−V). The hydrogen-bonding pattern surrounding the cystine knot is remarkably well conserved, including the β-bulge noted in hCG, NGF, and PDGF after Cys V (*31*).

The superpositions of the three dimers, as shown in Table 1, reveal that the overall structural similarity between neurotrophins is very high, about 1 Å in comparing positions of matched α-carbon atoms. This was to be expected, given the sequence alignment of human NT-3 with the other known human neurotrophins, as shown in Figure 2. Human NT-3 shares 57% amino acid identity with human NGF and 56% with human BDNF. Variable regions, in both sequence and structure, are present at the N- and C-termini, in the loops between the β-strands, and in the fourth β-strand. As might be anticipated from the evolutionary variety of residues in these loops and from looking at other neurotrophin crystal structures, we found a few of these loops to be variable in conformation and poorly ordered in the electron density maps, as discussed above. Other regions, including the critical six cysteines and the spacing between them, appear well conserved. As an aside, we note that human NT-6, which has been poorly characterized thus far, appears to lack one of the three disulfides (Figure 2). Removing a cysteine in Norrie disease protein, a cystine knot growth factor, destroys its function and causes an X-linked neurological disorder (*32*); how NT-6 compensates for the similar lack of cystine knot stabilization is unknown.

Dimer Interface. The dimer is stabilized by over 200 nonbonding interactions that bury 2110 Å^2 of hydrophobic surface area and 1250 Å^2 of polar and charged surface area. Table 2 summarizes these interfacial interactions for all the known neurotrophin structures and confirms that over a quarter of the NT-3 protomer's surface area is buried in the dimer interface. The amount of nonpolar surface area that is solvent inaccessible in the NT-3 protomer is low at 44.2%, which suggests a limited hydrophobic core. Upon dimerization, this rises to 55.7%, which is more typical of globular proteins. The formation of an extensive hydrophobic core is thought to help stabilize dimeric neurotrophins and cystine knot growth factor dimers (*5*).

Table 2: Interactions That Constitute the Neurotrophin Dimers[a]

interaction	NT-3	NGF	NT-3/BDNF
hydrogen bonds	10	7	8
van der Waals	200	100	140
contact surface area (Å^2)			
polar	1250	740	1030
apolar	2110	1800	2060
total	3360	2540	3090
total surface area (Å^2)	11490	11990	12360

[a] Hydrogen bonds were determined by the program HBPLUS (*41*); van der Waals interactions are contacts closer than 4.0 Å.

The residues that lie on the dimer interface are remarkably well conserved among the neurotrophins; this fact has been used to facilitate the manufacture of stable neurotrophin heterodimers (*33*). Heterodimers of NT-3 with NGF were not stable (*33*); this may be due to the significant differences in the polar and apolar makeup of NGF's and NT-3's dimer interfaces (Table 2). We compared the dimer interface structures of the NT-3 homodimer and the NT-3 heterodimer with BDNF (*12*). While the amount of buried surface area in proportion to total is slightly higher in the homodimer (29% versus 25%), the hydrophobic contribution is roughly the same in both. The homodimer and heterodimer have a similar number of side-chain-to-side-chain hydrogen bonds across the interface, though the actual residues involved are different. Our results show a striking overall similarity in

Table 3: Crystal Parameters, Data Collection, and Refinement Statistics

space group	$P2_12_12$
protein no. of residues/atoms	108/838
total reflections/unique reflections	20827/4535
average coverage of data from scaling	
all data	30−2.4 Å (85.3%)
highest resolution shell	2.5−2.4 Å (89.6%)
average redundancy of observations	4.6
R_{sym} (%)	5.5
molecular replacement	
R_{cryst}	41.6
correlation coefficient	59.7
refinement	
resolution range (Å)/	30−2.4/$F > 0\sigma$/4506
σ cutoff/reflections used	8.0−2.4/$F > 2\sigma$/4263
ordered waters seen	63
free *R*-factor (%)[a]	26.7
R-factor (%)[b]	23.3
bond rms deviation (Å)	0.007
angle rms deviation (deg)	1.56
protein mean *B*-factor (Å^2)	49.4
waters mean *B*-factor (Å^2)	53.7

[a] Free *R*-factor is the *R*-factor calculated only on the 10% of the reflections that were set aside for cross validation and not used in refinement. [b] *R*-factor $= \Sigma|F_o - F_c|/\Sigma|F_o|$.

the number of hydrogen bonds and in the distribution of buried surface area between the NT-3 homodimer and the BDNF/NT-3 heterodimer, which reinforces the notion that an evolutionarily conserved dimer interface probably resulted from the necessity for receptor dimerization in signal transduction.

Functional Implications. To gain insight into the structural determinants of binding to the Trk receptors and p75^{NTR}, several investigators have analyzed NT-3 and other neurotrophins using chimeric constructs, alanine scanning mutagenesis, and site-directed mutagenesis (*7*, *9*, *11*, *34*, *35*). These experiments suggest that NT-3 and NGF differ in the regions that confer receptor binding with affinity and specificity. In comparing NT-3 to NGF, residues have been identified that contribute little to binding affinity but much to binding specificity, and vice versa. In the case of NGF's binding to TrkA, a single structural feature most significantly contributes to both binding affinity and specificity, the N-terminal six residues (*36*). On the other hand, NT-3's residues involved in binding TrkC are not confined to one particular section but are distributed throughout the sequence. The key structural feature for binding to p75^{NTR} appears to be basic residues in region I or in region V, two loops that are spatially close (*34*) (Figure 2). Positively charged residues in these regions are conserved across the neurotrophins. We discuss below the structural features of the residues mediating binding affinity and binding specificity to TrkC and p75^{NTR}.

Urfer et al. analyzed surface residues of NT-3 for their contribution to binding affinity using alanine substitution mutants. Binding to TrkC was measured in vitro using binding competition assays with radioactive wild-type neurotrophin and using biological activity assays monitoring neurite growth in cell culture. When mutated to alanine, the residues identified as most significantly affecting binding to TrkC were Arg 103 (β-strand 4), Lys 80 and Gln 83 (β-strand 3), Arg 56 and Glu 54 (β-strand 2), and Thr 22 (β-strand 1) (*11*). Since our model represents an NT-3 homodimer, we can identify binding regions that involve both protomers, a task that could not be accomplished using the BDNF/NT-3 heterodimer structure, or an individual protomer. The residues mentioned above can be seen in our NT-3 model as creating a discrete binding face (Figure 3).

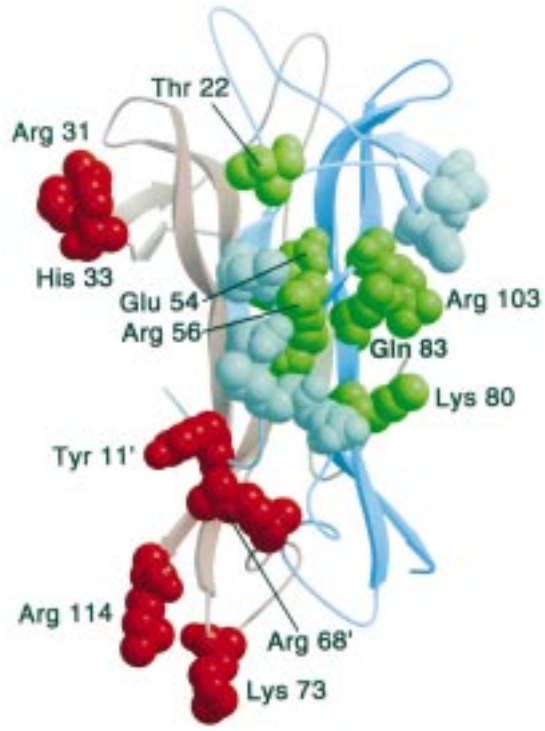

FIGURE 3: Residues involved in binding to TrkC and p75^{NTR} appear to form discrete patches, as shown by alanine scanning mutagenesis. When mutated to alanine, residues in green cause a significant loss of binding affinity to TrkC, those in orange cause a loss of binding affinity to p75^{NTR}, and those in gray caused no change in binding affinity to p75^{NTR} or TrkC. The two NT-3 protomers are shown in light red and blue.

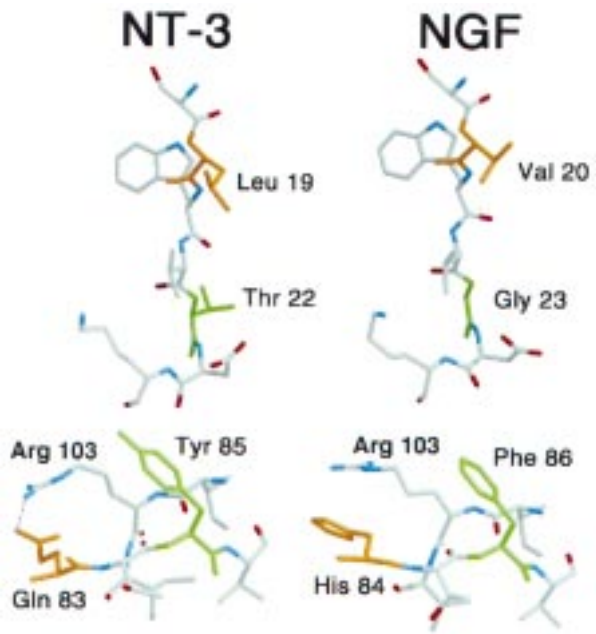

FIGURE 4: Four residues most important for TrkC specificity in NT-3 and their counterparts in NGF: (a, top) Thr 22 and Leu 19 in NT-3 compared to Gly 23 and Val 20 in NGF; (b, bottom) Gln 83 and Tyr 85 in NT-3 compared to His 84 and Phe 86 in NGF. Arg 103 is also shown in both NT-3 and NGF.

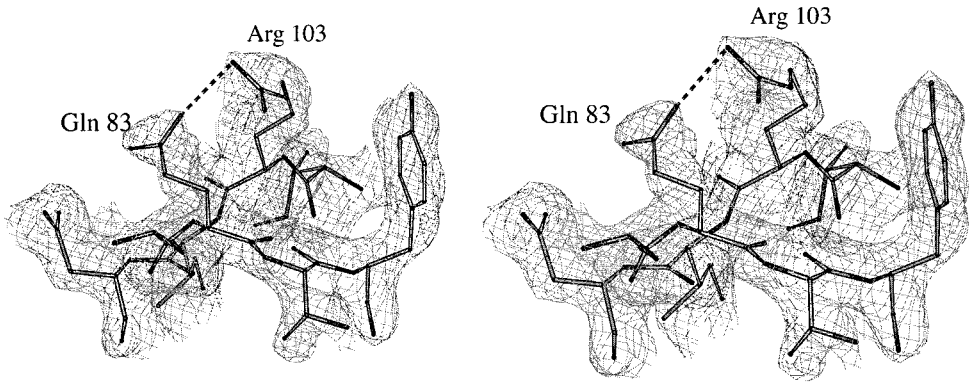

FIGURE 5: Stereoview of electron density in the region of Arg 103 and Gln 83. Shown is a $2F_o - F_c$ composite omit map, contoured at 1.0 σ and superimposed with the NT-3 homodimer model.

The data of Urfer et al. also help define a clearly marked boundary of residues that do not contribute to TrkC binding.

Discerning an analogous binding site on NT-3 for $p75^{NTR}$ is more difficult. Biological assays for $p75^{NTR}$ activity have not been performed; thus the only evidence for the interaction site is based on in vitro binding studies using radioactive wild-type neurotrophin competition. Nevertheless, residues were found (*11*) that form two discontinuous binding regions (Figure 3). One binding region involves residues Arg 31 and His 33, both in variable region I. More interestingly, a second region crosses both protomers; it is comprised of Tyr 11 and Arg 68 from one protomer and Lys 73 and Arg 114 from the other. This result suggests that the NT-3 dimer may be needed for $p75^{NTR}$ activation. All the residues implicated in binding $p75^{NTR}$ lie in mobile regions, either near the N- or C-termini or on one of the flexible loops. Strikingly, there is no overlap between the presumed binding regions for TrkC and $p75^{NTR}$. This is consistent with the curious observation that the presence of $p75^{NTR}$ improves neurotrophin binding to a Trk receptor (*37*), possibly by $p75^{NTR}$ initially binding the neurotrophin (*38*).

To identify the NT-3 residues most responsible for TrkC specificity, variants of NGF, formed by replacing four key residues with their NT-3 counterparts, were constructed that bind TrkC well and yet do not sacrifice TrkA binding (*35*). Two distinct regions on the β-sheet contain these critical specificity-lending residues. The first region lies near Thr 22 (Figure 4), the residue which Urfer et al. show is the most important for TrkC specificity. Substituting Thr 22 in place of the corresponding residue, a glycine, in NGF produces a 240-fold improvement in TrkC binding.[2] The addition of the hydroxyl moiety in threonine may allow a crucial hydrogen-bonding contact with the receptor. As was predicted by Urfer et al., one might expect that changing the Gly to Thr would significantly affect the backbone conformation, since glycine can tolerate greater flexibility. Surprisingly, this is not borne out in our NT-3 model, the backbone of which is exactly superimposable on NGF's in this region (Figure 4). This region also contains another important specificity-lending residue, Leu 19, which replaces Val 20 in NGF. The specificity here may be mediated by tight constraints on the side chain size or branching.

The second cluster of critical residues lies near Arg 103. Arg 103 is the most critical residue for binding affinity to TrkC; the corresponding residue in NGF, also an arginine, was shown to be insignificant for binding affinity to TrkA (*39*). Our results suggest that stabilization of this arginine in a unique conformation may represent a key feature of TrkC specificity. Significantly, the mutagenesis experiments of Urfer et al. show that Gln 83, which replaces His 84 in NGF, improves TrkC specificity. In our NT-3 model, the carboxyl group of the Gln 83 side chain accepts a hydrogen bond from the side chain of Arg 103 (Figure 4); this pulls the Arg side chain into a dramatically different position than is seen in NGF, which lacks such stabilization. Finally, Tyr 85 in NT-3 is important for TrkC specificity when it replaces Phe 86 in NGF. Tyr 85 in our model is directly adjacent to Arg 103, again highlighting the importance of this region for binding specificity. Tyr 85 is also the only of these four residues that lies in a hydrophobic cluster in the dimer interface. Mutation of Phe 86/His 84 to Tyr 85/Gln 83 in NGF may direct the molecule to a conformation more suitable for TrkC binding because of reorientation of Arg 103 and other side chains in this region.

In summary, we determined the X-ray crystal structure of the NT-3 homodimer. Clues to the specificity of NT-3 for its TrkC receptor were found when the structure was compared to NGF at functionally important residues. These clues suggest that both rigid and flexible regions are important for binding affinity and specificity. Rigid regions, such as the critical structures in the area of Arg 103 and the constant backbone structure near Thr 22 (Figure 4), likely represent scaffold areas that mediate binding to the TrkC receptor. Flexible loop regions, on the other hand, make up the binding site for $p75^{NTR}$ (Figure 3), which binds all the neurotrophins equally. TrkC specificity may depend on a hydrogen bond between Arg 103, the residue most crucial for binding affinity, and Gln 83, a residue very important for binding specificity. In addition, our results reveal that the dimer interface of the NT-3 homodimer is extensive and nonpolar, which may explain why dimerization is required for this molecule to exist. The similarity of interfacial hydrophobic contacts and hydrogen-bonding patterns between the NT-3 homodimer and those of the BDNF/NT-3 heterodimer helps to substantiate the view that this well-conserved dimer interface resulted from the requirement for receptor dimerization in signal transduction. Finally, combined with the recent Trk receptor mutagenesis results of Urfer et al. (*40*), crystallization of the Trk receptors (M. J. Butte et al., unpublished) with the neurotrophins promises

[2] Analogous NT-3 and NGF residues differ in numbering by one until residue 94, as shown in Figure 2.

to further define and confirm the interactions indicated.

ACKNOWLEDGMENT

We thank George D. Yancopoulos of Regeneron Pharmaceuticals, Inc., Tarrytown, New York, for generously providing the neurotrophin-3. M.J.B. acknowledges Andy Shiau and the UCSF Macromolecular Structure Group for helpful discussions.

REFERENCES

1. Kaplan, D. R., and Miller, F. D. (1997) *Curr. Opin. Cell Biol. 9*, 213-21.
2. Levi-Montalcini, R., Skaper, S. D., Dal Toso, R., Petrelli, L., and Leon, A. (1996) *Trends Neurosci. 19*, 514−520.
3. Yuen, E. C., and Mobley, W. C. (1996) *Ann. Neurol. 40*, 346−354.
4. Ryden, M., Sehgal, R., Dominici, C., Schilling, F. H., Ibanez, C. F., and Kogner, P. (1996) *Br. J. Cancer 74*, 773−779.
5. Sun, P. D., and Davies, D. R. (1995) *Annu. Rev. Biophys. Biomol. Struct. 24*, 269−291.
6. White, F. A., Silos-Santiago, I., Molliver, D. C., Nishimura, M., Phillips, H., Barbacid, M., and Snider, W. D. (1996) *J. Neurosci. 16*, 4662−4672.
7. Ilag, L. L., Lonnerberg, P., Persson, H., and Ibanez, C. F. (1994) *J. Biol. Chem. 269*, 19941−19946.
8. Persson, H., and Ibanez, C. F. (1993) *Curr. Opin. Neurol. Neurosurg. 6*, 11−18.
9. Ryden, M., and Ibanez, C. F. (1996) *J. Biol. Chem. 271*, 5623−5627.
10. Ibanez, C. F., Ilag, L. L., Murray-Rust, J., and Persson, H. (1993) *EMBO J. 12*, 2281−2293.
11. Urfer, R., Tsoulfas, P., Soppet, D., Escandon, E., Parada, L. F., and Presta, L. G. (1994) *EMBO J. 13*, 5896−5909.
12. Robinson, R. C., Radziejewski, C., Stuart, D. I., and Jones, E. Y. (1995) *Biochemistry 34*, 4139−4146.
13. Robinson, R. C., Radziejewski, C., Stuart, D. I., and Jones, E. Y. (1996) *Protein Sci. 5*, 973−977.
14. Kelly, J. A., Singer, E., Osslund, T. D., and Yeates, T. O. (1994) *Protein Sci. 3*, 982−983.
15. Otwinowski, Z., and Minor, W. (1996) in *Methods in Enzymology, Vol. 276, Macromolecular Crystallography* (Carter, C. W., Jr., and Sweet, R. M., Eds.) pp 307−326, Academic Press, New York.
16. Bailey, S. (1994) *Acta Crystallogr., Sect. D: Biol. Crystallogr. 50*, 760−763.
17. Navaza, J. (1994) *Acta Crystallogr., Sect. A: Found. Crystallogr. A50*, 157−163.
18. Brunger, A. T. (1988) *J. Mol. Biol. 203*, 803−816.
19. Muller, K., Amman, H. J., Doran, D. M., Gerber, P. R., Gubernator, K., and Schrepfer, G. (1988) *Bull. Soc. Chim. Belg. 97*, 655−667.
20. Adams, P. D., Pannu, N. S., Read, R. J., and Brunger, A. T. (1997) *Proc. Natl. Acad. Sci. U.S.A. 94*, 5018−5023.
21. Abrahams, J. P., and Leslie, A. G. W. (1996) *Acta Crystallogr., Sect. D: Biol. Crystallogr. 52*, 30−42.
22. Jones, T. A. (1992) in *Molecular Replacement* (Dodson, E. J., Gover, S., and Wolf, W., Eds.) pp 91−105, SERC Daresbury Laboratory, Warrington, U.K.
23. McDonald, N. Q., Lapatto, R., Murray-Rust, J., Gunning, J., Wlodawer, A., and Blundell, T. L. (1991) *Nature 354*, 411−414.
24. Holland, D. R., Cousens, L. S., Meng, W., and Matthews, B. W. (1994) *J. Mol. Biol. 239*, 385−400.
25. Eisenhaber, F., Lijnzaad, P., Argos, P., Sander, C., and Scharf, M. (1995) *J. Comput. Chem. 16*, 273−284.
26. Kraulis, P. J. (1991) *J. Appl. Cryst. 24*, 946−950.
27. Merritt, E. A., and Murphy, M. E. P. (1994) *Acta Crystallogr., Sect. D: Biol. Crystallogr. 50*, 869−873.
28. Nicholls, A., Sharp, K. A., and Honig, B. (1991) *Proteins 11*, 281−296.
29. Barton, G. J. (1993) *Protein Eng. 6*, 37−40.
30. Kleywegt, G. J., and Jones, T. A. (1994) *ESF/CCP4 Newsl. 31*, 9−14.
31. McDonald, N. Q., and Hendrickson, W. A. (1993) *Cell 73*, 421−424.
32. Strasberg, P., Liede, H. A., Stein, T., Warren, I., Sutherland, J., and Ray, P. N. (1995) *Hum. Mol. Genet. 4*, 2179−2180.
33. Radziejewski, C., and Robinson, R. C. (1993) *Biochemistry 32*, 13350−13356.
34. Ryden, M., Murray-Rust, J., Glass, D., Ilag, L. L., Trupp, M., Yancopoulos, G. D., McDonald, N. Q., and Ibanez, C. F. (1995) *EMBO J. 14*, 1979−1790.
35. Urfer, R., Tsoulfas, P., O'Connell, L., and Presta, L. G. (1997) *Biochemistry 36*, 4775−4781.
36. Shih, A., Laramee, G. R., Schmelzer, C. H., Burton, L. E., and Winslow, J. W. (1994) *J. Biol. Chem. 269*, 27679−27686.
37. Mahadeo, D., Kaplan, L., Chao, M. V., and Hempstead, B. L. (1994) *J. Biol. Chem. 269*, 6884−6891.
38. Bothwell, M. (1995) *Annu. Rev. Neurosci. 18*, 223−253.
39. Guo, M., Meyer, S. L., Kaur, H., Gao, J. J., and Neet, K. E. (1996) *Protein Sci. 5*, 447−455.
40. Urfer, R., Tsoulfas, P., O'Connell, L., Hongo, J. A., Zhao, W., and Presta, L. G. (1998) *J. Biol. Chem. 273*, 5829−5840.
41. McDonald, I. K., Naylor, D. N., Jones, D. T., and Thornton, J. M. (1993) HBPLUS, Department of Biochemistry and Molecular Biology, University College, London.

BI981254O